

Light-by-Light Scattering in a Photon-Photon Collider

T. Takahashi*

*Graduate School of Advanced Sciences of Matter, Hiroshima University,
1-3-1 Kagamiyama, Higashi Hiroshima, Hiroshima 739-8530, Japan*

G. An, Y. Chen, W. Chou, Y. Huang, W. Liu, J. Lv, G. Pei, S. Pei, and C. Zhang
Institute of High Energy Physics, Chinese Academy of Sciences, Beijing 100049, China

C. Zhang

*Key Laboratory of Beam Technology and Materials Modification of the Ministry of Education,
and College of Nuclear Science and Technology, Beijing Normal University, Beijing 100875, China*

W. Lu

Department of Engineering Physics, Tsinghua University, Beijing 100084, China

C. P. Shen and B. H. Sun

School of Physics and Nuclear Energy Engineering, Beihang University, Beijing 100191, China

(Dated: November 15, 2018)

We studied a feasibility of observing the light-by-light scattering in a photon-photon collider based on an existing accelerator complex and a laser system which can be commercially available. We investigated a statistical significance of the signal over the QED backgrounds through a Monte Carlo simulation with a detector model. The study showed that the light-by-light scattering can be observed with the statistical significance of 9 sigma in a year of operation.

PACS numbers: 14.70.Bh, 07.05.Fb

I. INTRODUCTION

Quantum electrodynamics (QED) is one of the most successful theory that describes the electromagnetic interaction and has been tested with great precision. Although the QED is a well-validated theory that underwent many experimental verifications, not all of its predictions have been observed to date. One of such areas is the interaction between real photons. Although the interactions between photons have been tested with great precision, all or a part of the photons involved in these interactions have been virtual photons. For example, the electron-positron pair creation caused by a photon impinging to the media, which is one of the most famous and well-tested process in the QED, is an interaction between a real photon and electric fields in media, characterizing a virtual photon. The only experimental observation of the pair creation by real photons was through the nonlinear QED interaction, performed by the E144 experiment in SLAC [1]. Another phenomenon of interest is light-by-light scattering. A higher-order perturbation of the QED predicts an elastic scattering between two photons. This phenomena has been known since the conception of the QED and the cross-section was calculated approximately 50 years ago[2, 3]. While several attempts to observe this phenomenon have been performed, no observation has been reported to date [4, 5]. An experimental observation of the process in heavy-ion collisions at the LHC

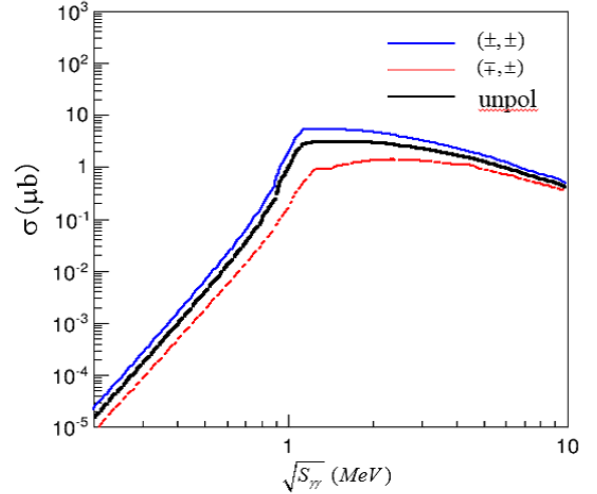


FIG. 1. The cross-section of the process, $\gamma\gamma \rightarrow \gamma\gamma$, by the collision of circularly polarized photons. (\pm, \pm) and (\pm, \mp) stand for the combination of the helicities of two colliding photons.

has been reported by the ATLAS experiment in 2017 [6, 7]; however, the direct observation in collisions of real photons remains to be reported.

Recently, experiments to probe the light-by-light scattering were proposed [8, 9]. Both of them utilized the laser-Compton scattering to generate photons at the center-of-mass energy range of approximately 1 MeV,

* tohru-takahashi@hiroshima-u.ac.jp; Corresponding author

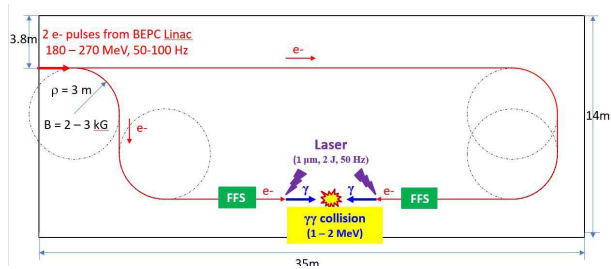


FIG. 2. A layout of the $\gamma\gamma$ collider facility in the IHEP experimental hall 10

where the cross-section of the light-by-light scattering is at the maximum as shown in fig. 1. In [8], the authors proposed an accelerator-based laser Compton facility; however, their proposal has not been approved. In [9], the authors plan to use a laser-plasma accelerator to provide an electron beam for Compton scattering. It may be a good opportunity to perform this kind of experiments, but the electron beam facility with laser-plasma acceleration remains to be developed. It must be pointed out that, in both proposals, the feasibility of observation of light-by-light scattering over possible backgrounds considering a detector response has not been fully studied.

In this article, we report on the feasibility of observations of the light-by-light scattering through a Monte Carlo simulation study considering most of the issues, such as background processes, following a detector model and a design of a photon-photon collider based on Beijing Electron Positron Collider (BEPC) accelerator complex in IHEP, China.

II. PHOTON-PHOTON COLLIDER

A planned layout of the experimental facility in an IHEP experimental hall is illustrated in fig. 2.

The electron beams from the BEPC linac was introduced to the hall and divided into two arcs, and subsequently brought into a head-on collision at the interaction point (IP). The laser pulses are flashed onto the electron beams at the conversion points (CP) shortly before they cross the IP, in order to generate photon beams. The main parameters of the electron and laser beams are summarized in table I.

We plan to use a photo-injector for the electron source to provide a low-emittance beam. The laser system is assumed to be 0.4–2 J/pulse with a width of 2 ps in the RMS and a repetition rate of 100 Hz. Due to a reason described later, the luminosity of the photon-photon collision must be tuned to optimize the detector performance, and we currently assume a laser pulse with 0.4 J/pulse, which is within the scope of a laser system commercially available at the moment. The differential luminosity calculated by using CAIN 2.42 [10] is shown in fig. 3. The total luminosity of photon-photon collision

TABLE I. The laser and the electron beam parameters for the proposed $\gamma\gamma$ collider. The size and pulse length of the laser pulse were defined as the RMS of the intensity.

Laser	Electron		
Wave length (μm)	1.054	Energy (MeV)	245
Size at focus (μm)	5	Bunch charge (nC)	1.25
Rayleigh Range (μm)	300	Size of IP (μm)	2
Pulse energy (J)	2 (0.4)	emittance (μm)	5.2×10^{-3}
Pulse Length (ps)	2	beta* at IP (mm)	727
Repetition (Hz)	100	bunch length (mm)	0.6
Angle (mr) to e-beam	167	Repetition (Hz)	100
IP-CP distance (mm)	383	crossing angle (mr)	0
Nonlinear parameter	0.3(2J)		

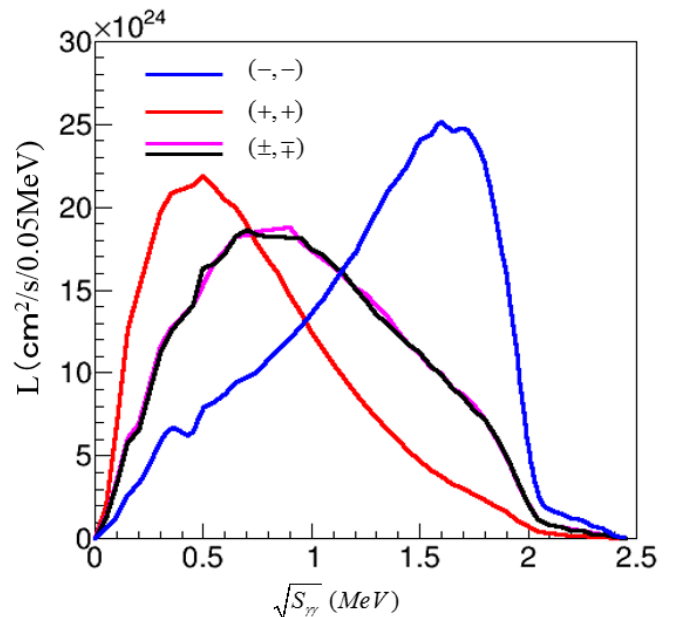


FIG. 3. The differential luminosity calculated by CAIN with the parameters shown in table I.

is approximately $4.0 \times 10^{27} \text{cm}^{-2} \text{s}^{-1}$ for the laser pulse energy of 2 J.

A. The Interaction region and detector

Fig. 4 illustrates the interaction region of the detector. We assumed a Final Focus system which consists of three permanent magnets, similar to that discussed in the reference [8]. The final focus magnet is placed at 10 cm from the IP. The inner and the outer radius of the magnet is 3 mm and 50 mm, respectively. To introduce laser pulses to the electron beam, the magnets have holes of 137 mr in angular aperture centered at 78 mr with respect to the beam axis and pointing to the IP. The angular aperture of the holes is approximately $\pm 4\sigma$ of the angular divergence of the laser wave to ensure good focusing property of the laser pulse the CP. the an The beam pipe, made

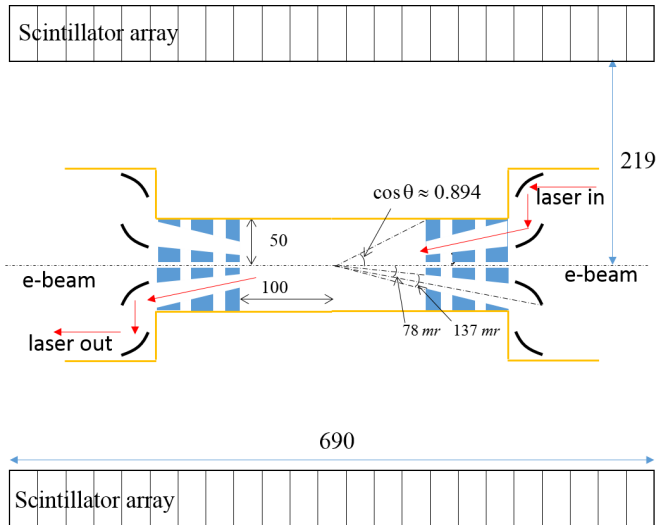


FIG. 4. The cross-sectional view of the detector model. The detector is a scintillator array made for the CsI and plastic scintillator. The final focus magnet of the radius of 50 mm is placed 100 mm from the interaction point. The laser pass (only one of the two) is indicated by arrows.

of 1-mm-thick beryllium, has an inner radius 50 mm so that the final focus magnets are placed within the beam pipe.

The detector is a calorimetric system with a scintillator array. Each module of the array consists of a 2-mm-thick plastic scintillator backed by a 60-mm-thick CsI crystal of a trapezoidal shape. The cross-section of the innermost surfaces (plastic scintillator) of the module is 30 mm \times 30 mm. The detector modules are arranged in a cylindrical shape along the beam axis. The number of modules is 23 in the beam direction, 46 in the plane perpendicular to the beam direction, and are 1058 in total (see fig. 4). The distance, R , of the front surface of the module from the IP is ;

$$R = \frac{w}{2 \tan \varphi/2} \approx 219.3 \text{ mm}$$

with w and φ being 30 mm and $2\pi/46$, respectively. The detector model was implemented in the Geant4 toolkit to simulate the detector response for the events[11]. After the simulation, the energy deposition in each detector module was smeared with a typical energy resolution (in the RMS) of the CsI and plastic scintillator as; $\frac{d\sigma}{E} = \frac{0.059}{\sqrt{E(\text{MeV})}}$ for the plastic and; $\frac{d\sigma}{E} = \frac{0.024}{\sqrt{E(\text{MeV})}}$ for the CsI scintillator, respectively.

III. EVENT RATE AND MONTE CARLO EVENT GENERATION.

To generate Monte Carlo (MC) events for the simulation study, the event rate N as a function of the polar

angle θ was calculated as;

$$\begin{aligned} \frac{dN}{d\theta}(\omega_{\gamma\gamma}, a_{\gamma\gamma}, h_{\gamma\gamma}) \\ = \frac{d\sigma_{\gamma\gamma}}{d\theta}(\omega_{\gamma\gamma}, h_{\gamma\gamma}) \frac{dL}{d\omega_{\gamma\gamma}}(\omega_{\gamma\gamma}, a_{\gamma\gamma}, h_{\gamma\gamma}) d\omega_{\gamma\gamma}, \end{aligned}$$

which is a function of the center-of-mass energy of colliding photon-photon system, $\omega_{\gamma\gamma}$, helicity combination of two photons, $h_{\gamma\gamma}$ and energy asymmetry of two photons, $a_{\gamma\gamma}$, where $h_{\gamma\gamma} = (+, +), (+, -), (-, +), (-, -)$ denotes the helicity combination of the two colliding photons and $a_{\gamma\gamma} \equiv \frac{e_1^1 - e_2^2}{e_1^1 + e_2^2}$ is the energy asymmetry of the two colliding photons. To perform the calculation, the differential luminosity; $\frac{dL}{d\omega_{\gamma\gamma}}(\omega_{\gamma\gamma}, a_{\gamma\gamma}, h_{\gamma\gamma})$ was estimated with CAIN in two-dimensional space in $\omega_{\gamma\gamma}$, $a_{\gamma\gamma}$ for each helicity combination, $h_{\gamma\gamma}$. The cross-section of the process $\gamma\gamma \rightarrow \gamma\gamma$, $\frac{d\sigma_{\gamma\gamma}}{d\theta}(\omega_{\gamma\gamma}, h_{\gamma\gamma})$, was calculated according to the formula given in the reference [2, 3] in the center-of-mass system and boosted to the laboratory system with the energy asymmetry $a_{\gamma\gamma}$. After these preparations, the Monte Carlo events were generated in five-dimensional phase space in $\theta, \varphi, \omega_{\gamma\gamma}, a_{\gamma\gamma}, h_{\gamma\gamma}$. As the background process for $\gamma\gamma \rightarrow \gamma\gamma$, we considered following processes;

- $\gamma\gamma \rightarrow e^+e^-$ Breit-Wheeler process
- $\gamma\gamma \rightarrow e^+e^-\gamma$ and $\gamma\gamma \rightarrow e^+e^-\gamma\gamma$ Breit-Wheeler process with the final state radiations
- $e^-\gamma \rightarrow e^-\gamma$ Compton scattering of a Compton photon and a beam electron
- $e^-\gamma \rightarrow e^+e^-e^-$ the trident process with a Compton photon and a beam electron
- $e^-e^- \rightarrow e^-e^-$ Moller scattering of beam electrons.

The Compton scattering between a beam electron and a Compton photon. $e^-\gamma \rightarrow e^-\gamma$, has a large cross-section; however, all final state particles will escape into the beam direction and does not contribute to the background. We adopted WHIZARD[12] for the cross-section calculations and subsequent event generations for background processes. The photon-photon, photon-electron, and electron-electron luminosity distributions were implemented to WHIZARD via its built-in utility program CIRCE2. The effective production cross-section was defined as;

$$\sigma_{eff} \equiv \frac{1}{L_{ij}^{tot}} \sum_{h_{ij}} \int \sigma(\omega_{ij}, h_{ij}) \frac{dL_{ij}}{d\omega_{ij}}(\omega_{ij}, h_{ij}) d\omega_{ij}.$$

In the above expression, the total luminosity is calculated using the results of CAIN as:

$$L_{ij}^{tot} \equiv \sum_{h_{ij}} \int \frac{dL_{ij}}{d\omega_{ij}}(\omega_{ij}, h_{ij}) d\omega_{ij}.$$

All cross-sections except for $\gamma\gamma \rightarrow \gamma\gamma$ were calculated with a kinematic cut, such that at least one final state

particle must be within the angular acceptance of the detector ($|\cos\theta| < 0.8944$) (see fig. 4). The calculated effective cross-section for each process is;

$$\begin{aligned}\sigma_{eff}(\gamma\gamma \rightarrow \gamma\gamma) &= 1.5\mu b \\ \sigma_{eff}(\gamma\gamma \rightarrow e^+e^-) &= 5.7 \times 10^4\mu b \\ \sigma_{eff}(\gamma\gamma \rightarrow e^+e^-\gamma) &= 4.7 \times 10^3\mu b \\ \sigma_{eff}(\gamma\gamma \rightarrow e^+e^-\gamma\gamma) &= 2.1 \times 10^2\mu b \\ \sigma_{eff}(e^-\gamma \rightarrow e^-\gamma) &= 8.9 \times 10^2\mu b \\ \sigma_{eff}(e^-\gamma \rightarrow e^+e^-e^-) &= 3.7 \times 10^3\mu b \\ \sigma_{eff}(e^-e^- \rightarrow e^-e^-) &= 2.1 \times 10^1\mu b\end{aligned}$$

In order to ensure proper detector operation and subsequent data analysis, we must suppress the event pileups in a bunch collision below a reasonable level. The number of events per bunch, N_b , can be expressed by the effective cross-section and the bunch luminosity as: $N_b = \sigma_{eff}L_b$. Assuming N_b for the $\gamma\gamma \rightarrow e^+e^-$, which has the largest cross-section, being 0.1,

$$L_b = 0.1/\sigma_{eff}(\gamma\gamma \rightarrow e^+e^-) \approx 1.3 \times 10^{24}cm^{-2}$$

According to the luminosity calculation with CAIN, bunch luminosity for 2J/pulse laser (in table I) is $\approx 4 \times 10^{25}cm^{-2}$. Thus, we must decrease the bunch luminosity by a factor of 30. It allows us to reduce, for example, laser power to about 0.4 J/pulse, leaving an appreciable margin for designing the entire system. Consequently, the expected number of events per second, by normalizing $N(\gamma\gamma \rightarrow e^+e^-) = 0.1/s$, is;

$$\begin{aligned}\sigma_{eff}(\gamma\gamma \rightarrow \gamma\gamma) &= 2.7 \times 10^{-4} \\ \sigma_{eff}(\gamma\gamma \rightarrow e^+e^-) &= 10 \\ \sigma_{eff}(\gamma\gamma \rightarrow e^+e^-\gamma) &= 8.3 \times 10^{-1} \\ \sigma_{eff}(\gamma\gamma \rightarrow e^+e^-\gamma\gamma) &= 3.7 \times 10^{-2} \\ \sigma_{eff}(e^-\gamma \rightarrow e^-\gamma) &= 0.3 \\ \sigma_{eff}(e^-\gamma \rightarrow e^+e^-e^-) &= 1.1 \\ \sigma_{eff}(e^-e^- \rightarrow e^-e^-) &= 2.5 \times 10^{-3}\end{aligned}$$

IV. DATA ANALYSIS

A. Analysis overview

The MC events are generated according the formula III. In fig. 5, we show the total energy deposition in the detector for $\gamma\gamma \rightarrow \gamma\gamma$ and $\gamma\gamma \rightarrow e^+e^-$ processes after the detector simulation described in section II A.

The peaks around 0.5 MeV and 1 MeV are observed for $\gamma\gamma \rightarrow e^+e^-$ events. These peaks are attributed to the annihilation of a positron in materials. As the center-of-mass energy of the $\gamma\gamma$ collision is near the threshold of pair creation, the momenta of the electron and positron of the order of a few hundred keV at most. Therefore,

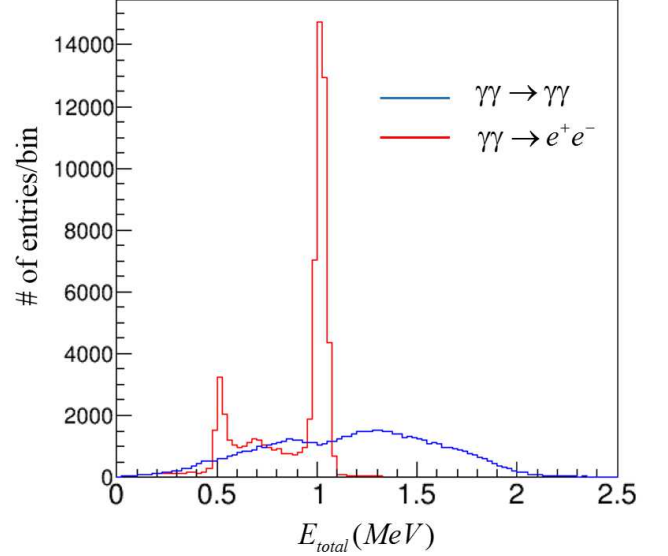


FIG. 5. Total energy deposition observed by the detector. Clear peaks caused by a positron annihilation in the materials for $\gamma\gamma \rightarrow e^+e^-$ process are observed; i.e., the peak around 1 MeV is represents the case where two 0.511 MeV photons are destructed, while the peak around 0.511 MeV is indicative of the case in which one of the two photon escapes from the detector.

virtually all electrons and positrons stop inside the material around the IP, even in the beam pipes of 1-mm-thick beryllium. When a positron stops in materials, it generates back-to-back photons of approximately 0.511 MeV. This phenomena resemble the signal events and its discrimination are crucial for the signal detection. It should be noted that because the event signatures of both processes are back-to-back photons, the identification of the charged particle will not help improve the situation. A typical $\gamma\gamma \rightarrow e^+e^-$ event observed in the detector is shown in fig. 6. Two photons are generated in back to back direction from a point in the beam pipe, where a positron is absorbed, while the electron absorbed in the beam pipe had no effect. In order to discriminate the background photons from the beam pile, and the signal from the IP, we increase the radius of the beam pipe to 50 mm so that these two processes can be discriminated from one another by defining proper observables, as described in section IV B.

B. Event analysis

We generated the MC events for signal and background processes. The number of event samples were, 2,100 k for $\gamma\gamma \rightarrow e^+e^-$, 1,100 k for $\gamma\gamma \rightarrow e^+e^-\gamma$ and $e^-\gamma \rightarrow e^+e^-e^-$, 200 k for the remaining signal and background processes. After simulating the detector response by Geant4, momentum vectors, \vec{p}_i , were defined for each

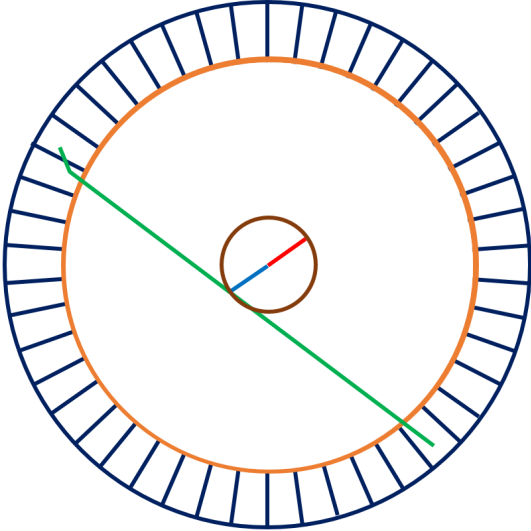


FIG. 6. Illustration of a typical $\gamma\gamma \rightarrow e^+e^-$ event. A positron is absorbed in the beam pipe and generates back to back photons.

hit in a detector module in an event as;

$$\vec{p}_i = E_i \vec{r}_i$$

where E_i is the energy deposition in i_{th} plastic or CsI module and \vec{r}_i is the position of the innermost surface of the module. With these vectors, two jets, $\vec{P}_{1(2)}$, which represent the final state particles for an event, were reconstructed by applying the forced two-jet clustering technique with the Dharum algorithm[13]. (\vec{P}_1 and \vec{P}_2 are chosen such that \vec{P}_1 is the jet of the higher energy.) For further analysis, the following observables are defined using \vec{P}_j as;

1. $E_j \equiv |\vec{P}_j|$; Energy of each jet;
2. $E = \sum E_j$; Total energy of an event deposition;
3. $\cos \theta_{P_1}$
4. $\cos \theta_{P_2}$
5. $\theta_{acl} \equiv \pi - \vec{P}_1 \angle \vec{P}_2$; acollinearity angle
6. $\theta_{acp} \equiv \pi - P_1^\perp \angle P_2^\perp$; acoplanarity angle
7. E_1^{psc} ; Energy deposition on the plastic scintillator of \vec{P}_1
8. E_2^{psc} ; Energy deposition on the plastic scintillator of \vec{P}_2

In the above expression, $\vec{P}_1 \angle \vec{P}_2$ stands for the opening angle of two vectors, \vec{P}_1, \vec{P}_2 .

The distribution of each observable for the signal and backgrounds event are shown in fig. 7. In order to discriminate between signal and backgrounds, we used

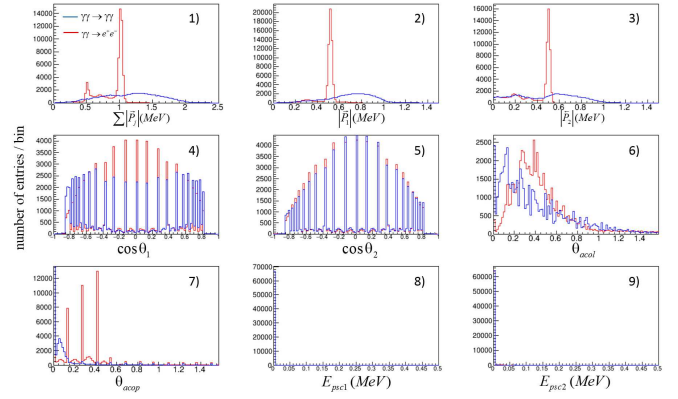


FIG. 7. Distributions of observables used for the analysis. For visualization purposes, the number of entries in each figure is a result of 100k simulated events and does not represent the expected number of events in the experiment. The numbers on each panel corresponds to definitions of valuables in the text.

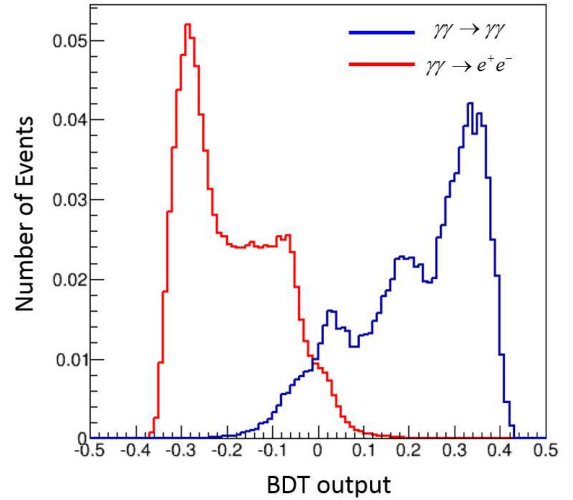


FIG. 8. BDT outputs for $\gamma\gamma \rightarrow \gamma\gamma$ (blue) and $\gamma\gamma \rightarrow e^+e^-$ (red) events. The figure demonstrate the differences in distributions such that the entries of the histogram for each process are normalized by the number of entries in the histograms.

the Boosted Decision Tree (BDT) technique implemented in the Toolkit for Multi-variable Analysis(TMVA) in ROOT[14]. For each signal and background events, 100 k events were used to train the BDT and remaining events were used to test the performance of the event selection. The outputs from the BDT analysis are shown in fig. 8. Using the number of events survived for the signal and the background, the expected statistical significance, sig is defined as;

$$sig \equiv \frac{N_S}{\sqrt{N_S + N_B}}$$

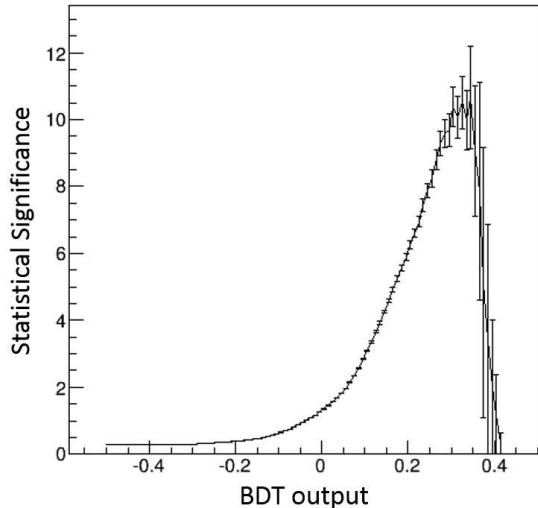


FIG. 9. Expected statistical significance of $\gamma\gamma \rightarrow \gamma\gamma$ signal over the background after one year of operation.

The significance was calculated with the expected number of events for a one-year operation (10^7 s) of the experiment. The calculated significance is plotted as a function of the BDT output in fig.9. The error in the plots is the statistical uncertainty of the MC events. The result shows that the statistical significance $\gamma\gamma \rightarrow \gamma\gamma$ over the background processes is expected to exceed 9 sigma after a year (10^7 s) of operation, which is well above the

significance regarded as discovery.

V. CONCLUSION

We demonstrated the feasibility of observing the light-by-light scattering in a photon-photon collider based on a design with existing facility and feasible technology. An expected statistical significance to observe the signal has been investigated for the first time with a realistic luminosity distribution estimated using an accelerator lattice and laser optics, a detector model that can be constructed using reasonable resources, and a Monte Carlo data analysis considering most of the possible background processes. The results showed that the light-by-light scattering can be observed with a statistical significance of 9 sigma after one year of operation, which is well above the level of discovery.

In addition to the observation of the light-by-light scattering, we note that the Breit-Wheeler process has not been observed by the collision of real photons. In addition, the proposed photon-photon collision system can be realized as a facility to observe non-linear effect in the QED, such as a shift in the high energy peak and/or multiple photon absorption in Compton scattering.

ACKNOWLEDGMENTS

This work is supported by National Natural Science Foundation of China (11655003), Innovation Project of IHEP (542017IHEPZZBS11820), and in part by the CAS Center for Excellence in Particle Physics (CCEPP).

-
- [1] C. Bamber, et.al, Phys. Rev. D60 092004 (1999).
 - [2] B. De Tollis, Nuovo Cimento 32, 757 (1964).
 - [3] B. De Tollis, Nuovo Cimento 35, 1182 (1965).
 - [4] F. Moulin, De. Bernard and F. Amiranoff, Z. Phys. C 72, 607 (1996).
 - [5] M. Marklund and J. Lundin, Eur. Phys. J. D 55, 319 (2009).
 - [6] D. d’Enterria and G. G. da Silveira, Phys. Rev. Letts. 111, 080405 (2013).
 - [7] ATLAS Collaboration, Nature Phys. 13, 852 (2017).
 - [8] D. Micieli, I. Drebot, A. Bacci, E. Milotti, V. Petrillo, M. R. Conti, A. R. Rossi, E. Tassi and L. Serafini, Phys. Rev. Acc. and Beams 19, 093401 (2016)
 - [9] K. Homma, K. Matsuura, and K. Nakajima, arXiv:1505.03630v2
 - [10] <https://ilc.kek.jp/yokoya/CAIN/Cain242/>, P. Chen, T. Ohgaki, A. Spitkovsky, T. Takahashi, and K. Yokoya, Nucl. Instr. Meth Phys. A 397, 458 (1997).
 - [11] S. Agostinelli, et.at, Nucl. Instr. and Meth. A 506 (2003) 250, J. Allison, et. at, IEEE Trans. on Nucl. Sci. 53 No. 1 (2006) 270, J. Allison, et. at, Nucl. Instr. and Meth. A 835 (2016) 186.
 - [12] W. Kilian, T. Ohl, J. Reuter, Eur.Phys.J.C71 (2011) 1742. M. Moretti, T. Ohl, J. Reuter, O’Mega, LC-TOOL-2001-040-rev, arXiv: hep-ph/0102195-rev.
 - [13] M. Cacciari, arXiv:hep-ph/0607071
 - [14] <https://root.cern.ch/>